LONGITUDINAL BEAM PROFILE MONITOR FOR INVESTIGATING THE MICROBUNCHING INSTABILITY AT DIAMOND LIGHT SOURCE*

W. Shields†, P. Karataev, JAI at Royal Holloway, Egham, UK
R. Bartolini, A. Morgan, G. Rehm, Diamond Light Source, Oxfordshire, UK

Abstract

An investigation into the microbunching instability at Diamond Light Source has recently been conducted. Beyond the instability threshold, the longitudinal distribution of the bunch starts filamenting. As a result, the bunch emits bursts of coherent synchrotron radiation with wavelengths shorter than the bunch length. The operating conditions for producing the instability include both standard optics, and low-alpha optics, where the bunch length can be shortened to a few picoseconds. A Michelson interferometer has been designed and installed utilising a silicon crystal wafer beamsplitter. Large bandwidth, room temperature pyroelectric detectors and low-noise, fast-response Schottky Barrier diode detectors have been employed to measure the interferograms. In this paper, we describe the observed results and calculated spectral content.

INTRODUCTION

The microbunching instability is a phenomenon which has been observed in many storage rings across the globe [1–5]. The instability is characterised by the onset of bursts of coherent synchrotron radiation with a wavelength of the order of the bunch length. At the threshold current, the bursting is quasi-periodic, however, at higher currents, the bursting exhibits a seemingly chaotic nature. The emissions' coherence indicates that the signal intensity is proportional to N^2, with N being the number of electrons in the bunch. This strong dependence on bunch current, along with other machine parameters, has been previously studied at Diamond Light Source [1,2,6], however these studies have been limited to experiments in instability detection. The machine conditions necessary to produce the instability at Diamond are well known; the instability has been created in standard optics while operating with a single high charge bunch, and additionally in a low-alpha lattice [6]. The low-alpha lattice operates with a first-order momentum compaction factor, $\|\alpha_1\| = 1 \times 10^{-6}$ [7], permitting the shortening of bunches to a few ps. However, the bunch's susceptibility to longitudinal instabilities limits the bunch current in the low-alpha setup to tens of μA, consequently limiting the storage ring performance.

The recent installation of a dedicated mm-wave diagnostic port has greatly improved our ability to conduct further investigations. Whilst previous tests at the port focussed on viewport characterisation and instability detection, a Michelson interferometer has been installed with the purpose of measuring the longitudinal beam profile. The interferometer permits measurements of the emitted spectrum arising as a result of the instability, which we can consequently use to calculate the bunch length. In this paper, we present a series of measurements from the interferometer, from operation of both standard and low-alpha optics.

EXPERIMENTAL SETUP

The interferometer setup was installed at the dedicated mm-wave diagnostic port, with radiation produced from bunches passing through bending magnet B06. The port comprises of a water cooled copper mirror to absorb high intensity X-rays, and a second mirror to reflect the radiation into a plane that is parallel to, but vertically lower than the beampipe. The port window is a 89 mm diameter, 6mm thick fused silica window providing very little absorption in the mm-wave region of the electromagnetic spectrum. Spatial constraints have resulted in the inclusion of several mirrors in the radiation transfer line. Figure 1 shows the experimental setup, with the radiations direction of propagation indicated by the yellow arrows. The beams angle of incidence can be manipulated using components A and B, a 3 dimension position controlled mirror, and an actuator controlled mirror respectively. The interferometer is comprised of: component C, a crystal silicon wafer beamsplitter; D, a fixed mirror; E, a linearly translatable mirror with 150mm range; F, a flat, fixed mirror; G, a parabolic mirror included to focus the beam; and component H, the detector. Two silicon beamsplitters were employed in separate experiments, the first being $\sim$160 μm thick, and the second being $\sim$ 100 μm thick. The change of splitter is explained later in this paper.

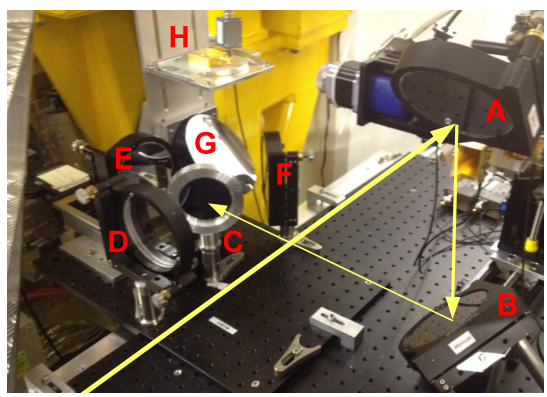

Figure 1: Interferometer Setup.

* The research leading to these results was funded by Diamond Light Source and by STFC
† william.shields.2010@live.rhul.ac.uk

ISBN 978-3-95450-127-4

Table 1: Detector Specifications

Detector	Quasi-Optical Schottky Diode	Pyroelectric
Frequency Range (GHz)	100 - 1000	100 - 30,000+
Wavelength (mm)	3 - 0.3	3 - 0.01
Responsitivity (V/W)	500	7×10^4
Noise Equivalent Power ($pW/\sqrt{Hz}$)	10	1000

Two detectors were employed in the setup in separate experiments: a low noise, fast-response quasi-optical Schottky Barrier Diode detector from Virginia Diodes, and a large bandwidth, room temperature pyroelectric detector from Gentec-EO. A specification comparison of the two detectors is shown in table 1. The use of the pyroelectric detector subsequently required the installation of a chopper to modulate the beam. A styrofoam sheet was additionally included in the setup to absorb the shorter wavelength incoherent infrared signal which is detectable by the pyroelectric detector. The detector outputs were connected to a lock-in amplifier with the chopper as the reference source. The movable arm of the interferometer was controlled remotely with steps of selectable size moved over a chosen scan length around the point of zero path difference. A 20 sample average and standard deviation were recorded for each step in the interferogram scan. The spectral content of the emissions were obtained by fast-fourier transform of the interferograms in post-experimental analysis with any recorded spectra normalised to the square of the bunch current and the number of bunches. In early tests, a small but noticeable interferometer misalignment was corrected by normalising to a linear fit of the scan.

STANDARD OPTICS RESULTS

For the experiments under standard optics, Diamond was operated in either a single or two bunch fill pattern. Whilst the bunch length can be shortened by increasing RF voltage, the standard optics setup in user configuration maintains a constant 2.5 MV. Diamond uses two superconducting RF cavities operating at $\sim$ 500 MHz RF frequency with cavities set at 1.1 and 1.4 MV. During all interferogram scans, the voltage experienced by the bunches was assumed to be the sum of the voltages from both cavities.

Figure 2 shows the interferograms recorded from the pyroelectric detector (2a) and the quasi-optical detector (2b), with the measured standard deviation shown as voltage error. Both detectors show an interference pattern with a typical maxima separation of $\sim$ 2mm and path difference interference extent of $\pm$ 15mm. The path difference is limited to this range as part of the data analysis; the continuous incoherent signal generates noise of sufficient amplitude throughout the scan to contribute noise to the corresponding spectrum; therefore reduction of scanning range, whilst lowering the frequency resolution, provides a reduced-noise spectrum. Notably, the quasi-optical scan appears to display a zero path difference at a point of destructive interference. The results from the quasi-optical detector unusually showed a longer wavelength modulation to the signal throughout the entire scanning range of the movable arm of the interferometer. Further investigations at the 2.5 MV RF voltage revealed that the modulation is not limited to the region around the point of zero-path difference, therefore, it is thought to be the results of a standing wave between two components of the apparatus, and will consequently add a substantial low-frequency component to the spectrum. The signal recorded throughout the full scan range was used to remove this modulation, and can be attributed as the cause of the displayed interferogram anomaly.

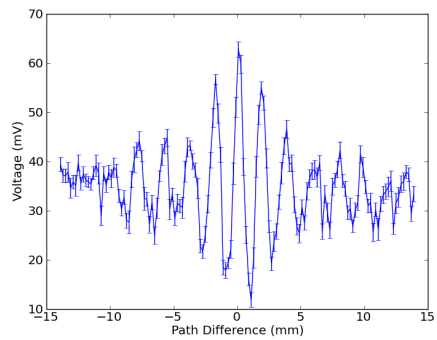

(a)

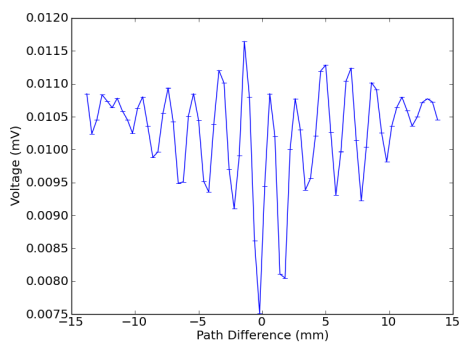

(b)

Figure 2: Interferograms from user mode operation with the pyroelectric detector (2a), and the quasi-optical detector (2b) with removed modulation.

The corresponding spectra from the two interferograms in Fig. 2 are shown in Fig. 3. The two spectra both show a signal between $\sim$ 140 GHz and 200 GHz, however limited

ISBN 978-3-95450-127-4

comparisons can be drawn due to the length of the spectra; Fig. 3b has a significantly shorter spectra due to a larger interferogram step size.

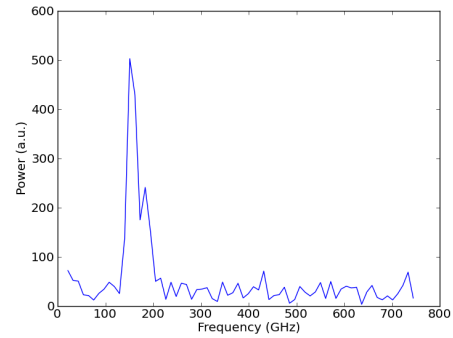

(a)

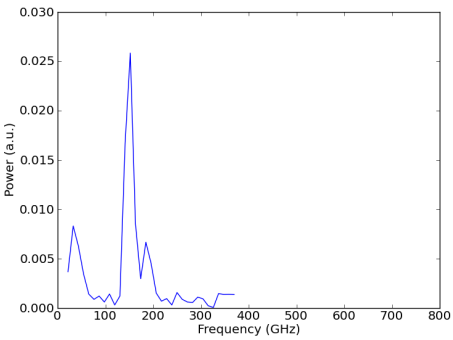

(b)

Figure 3: Measured spectrum from the pyroelectric detector (3a), and the quasi-optical detector (3b) from user mode operation.

LOW ALPHA RESULTS

The measurements of the signal from the low-alpha lattice by the pyroelectric and quasi-optical detectors are shown in Fig. 4. An RF voltage of 2.5 MV was maintained for the low-alpha experiments, however the pyroelectric detector experiment was operated with 1.25 MV in each cavity as opposed to the standard setup. Time constraints during the experiments prevented a more detailed comparison, consequently producing the difference in scan length.

There are clear differences in the symmetry and interferogram amplitude. Whilst the scan range significantly contributes to the apparent decreased width, the interference pattern appears to be approaching the background non-interference signal voltage at the positions furthest from the point of zero path difference. The pyroelectric interferogram in Fig. 4a shows excellent symmetry suggesting a stable, coherent source of mm-wave radiation. However, the quasi-optical detectors asymmetry is indicative of unstable bursting. The disparity between the two interferograms is potentially a result of different step sizes within the scans; a

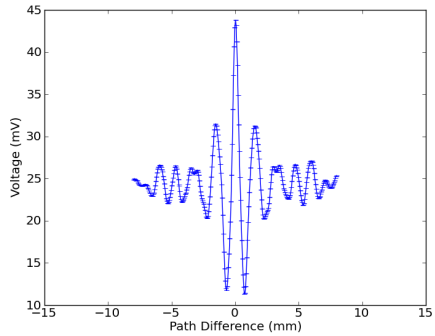

(a)

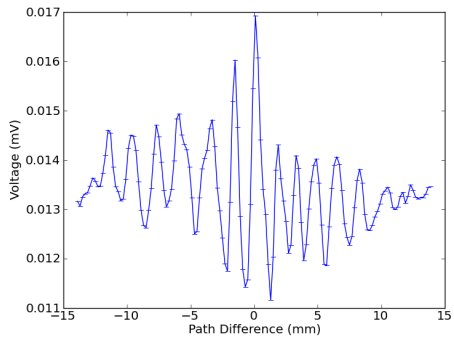

(b)

Figure 4: Interferograms from low-alpha optics with the pyroelectric detector (4a), and the quasi-optical detector (4b)

factor of four larger step size in the quasi-optical scan may have resulted in an aliasing of the signal despite the small standard deviation of the measured data.

The controllable mirrors in the radiation transfer line may have introduced an additional misalignment effect. Minor alterations to the setup during the storage rings shutdown periods resulted in continuous scans with the transfer line mirrors to seek the optimum position for peak power. These adjustments potentially added a small angular deviation to the signal path, which, in combination with the path length to the detector and wavelength range of the incident beam, could explain the lack of interferogram symmetry in the later experiments. Further investigations are needed to provide a conclusive explanation.

The disparity of the interferograms is consequently observed in the calculated spectrum, as seen in Fig 5. The spectrum from the pyroelectric detector in Fig. 5a reveals signal at frequencies up to 650 GHz, a result of the shorter bunch length from low-alpha operation producing coherent signal at shorter wavelengths. The asymmetry within the quasi-optical test results in a 'rough' spectrum, where many unexpected dips in spectral power are observed. The lack of power in some frequency regions is also observable in the pyroelectric detector spectrum, notably at $\sim$ 300 GHz. Theoretical calculations of the Fresnel reflection and trans-

ISBN 978-3-95450-127-4

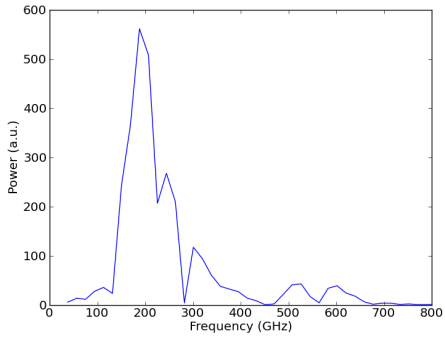

(a)

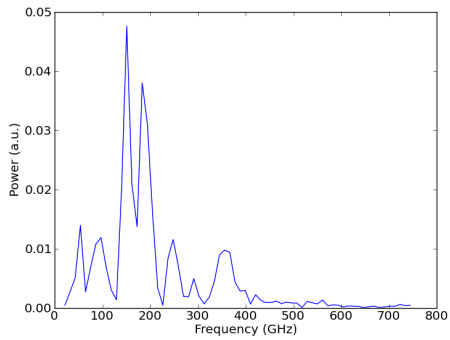

(b)

Figure 5: Measured spectrum from the pyroelectric detector (5a), and quasi-optical detector (5b) from the low-alpha setup.

mission coefficients, for crystalline silicon at a 45 degree incidence angle, revealed an absence of these frequencies was the result of a drop in efficiency of the 160 μm thick beamsplitter, as shown in Fig. 6. Additional calculations concluded that a 100 μm thick splitter increases the frequency of the reduced efficiency such that the calculated spectrum is not adversely affected. The thinner beamsplitter was installed prior to the quasi-optical detector, however the efficiency drop cannot be identified due to lack of high frequency signal in the case of standard optics, and the less well defined spectrum from low-alpha.

The calculated spectra in Fig. 3 and 5 all exhibit a sharp low frequency cutoff at around 140 GHz. The repetition of the cutoff at this frequency suggests the presence of a cutoff in the interferometer setup which requires further analysis.

From the recorded spectra, and from the responsivity specification in tab. 1, we can provide an approximation of detected signal power and signal-to-noise ratio. Under standard optics, the estimated power from the pyroelectric and quasi-optical detectors is 500 nW and 20 nW respectively, and from the low-alpha optics, the power is 350 nW and 27 nW respectively. The order of magnitude difference is potentially due to the large bandwidth of the pyroelectric detector; the detector is sensitive to frequencies much higher than the interferometer is capable of resolving. Further investigation of the detectors and possible filtering mechanisms is required. The smallest corresponding signal-to-noise ratio can be estimated to be 350 for the pyroelectric detector, and 2000 for the quasi-optical detector. The non-uniformity of the detector's responsivity with frequency, and estimation of average signal voltage prevents any exact conclusions regarding the signal power disparity, however the difference in signal to noise ratio is expected as a result of the low noise of the quasi-optical detector.

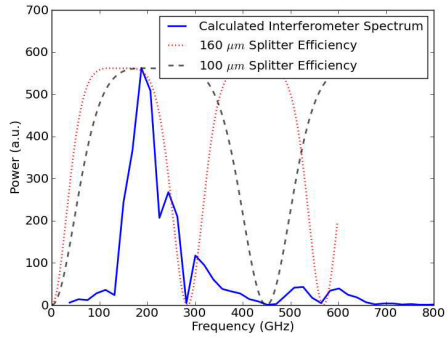

Figure 6: Calculated low-alpha spectrum and normalised theoretical silicon beamsplitter efficiencies.

CONCLUSIONS AND FUTURE WORK

We have presented the first results from a CSR-based longitudinal beam profile monitor. Experiments conducted using a Michelson interferometer with a pyroelectric detector and quasi-optical detector successfully produced preliminary spectra from the microbunching instability in electron bunches from both a normal and a low-alpha optics setup. Both setups revealed a strong signal between 140 and 200 GHz, with the low-alpha experiments displaying spectral emissions up to 650 GHz. The efficiency of the interferometer's initial beamsplitter was shown to partially block the spectrum, but theoretical calculations have shown that the second, thinner splitter should alleviate this limitation.

Further analysis and investigation is required to explain the frequency domain irregularities in order to provide a spectrum suitable for calculation of the bunch length.

REFERENCES

[1] G. Rehm et al., DIPAC 2009, TUPD32.

[2] W. Shields et al., *J. Phys. Conf. Ser.* **357**, 012037, (2012).

[3] J.M Byrd et al., *Phys. Rev. Lett.* **89**, 224801, (2002).

[4] M. Ako-Bakr et al., *Phys. Rev. Lett.* **88**, 254801, (2002).

[5] G. Wüstefeld, EPAC 2008, MOZAG02.

[6] W.Shields et al., IPAC 2012, WEPPR079.

[7] I.P. Martin et al., *Phys. Rev. STAB.* **14**, 040705, (2011).

ISBN 978-3-95450-127-4